Optics Communications 284 (2011) 3134–3139

Contents lists available at ScienceDirect

Optics Communications

journal homepage: www.elsevier.com/locate/optcom

Tunneling-induced coherent electron population transfer in an asymmetric quantum well

Ni Cui [a], Yueping Niu [a,*], Shangqing Gong [b,*]

[a] State Key Laboratory of High Field Laser Physics, Shanghai Institute of Optics and Fine Mechanics, Chinese Academy of Sciences, Shanghai 201800, China
[b] Department of Physics, East China University of Science and Technology, Shanghai 200237, China

ARTICLE INFO

Article history:
Received 1 September 2010
Received in revised form 21 February 2011
Accepted 22 February 2011
Available online 9 March 2011

Keywords:
Quantum well
Coherent population transfer
Resonant tunneling
Fano interference

ABSTRACT

We propose an asymmetric double quantum wells structure with a common continuum and investigate the effect of resonant tunneling on the control of coherent electron population transfer between the two quantum wells. By numerically solving the motion equations of element moments, the almost complete electron population transfer from the initial subband to the target subband could be realized due to the constructive interference via flexibly adjusting the structure parameters.

1. Introduction

Coherent population transfer among discrete quantum states in atoms and molecules has attracted tremendous attentions [1,2] over the past few decades, due to its potential application to atomic optics [3], preparation of entanglement [4] and superposition states[5,6], and quantum computation [7]. The most robust technique for achieving efficient population transfer is stimulated Raman adiabatic passage (STIRAP) [1,2,8,9], by which perfect population transfer has been studied in a three-level Λ system particularly. Moreover, the case when the upper isolated discrete level is replaced with a continuum was suggested initially by Carroll and Hioe [10]. In their model, the continuum could serve as an intermediary for population transfer between two discrete states in an atom or a molecule by STIRAP. Later, Nakajima et al. [11] have shown that complete population transfer is impossible in realistic mode with continuum intermediate states. However, significant partial transfer may still be feasible theoretically [12–16] and experimentally [17]. Further, the possibility to achieve complete adiabatic population transfer is examined in the case when the single intermediate state in STIRAP is replaced by N states [18,19]. In particular, Gong et al. [20] demonstrated that a complete population transfer from an initial state to another target state and an arbitrary superposition of atomic states could be realized with the STIRAP technique in an excited-doublet four-level atom systems. Lately, considering the same system with spontaneous decay-induced coherence, Zhu et al. [21] investigated that the remarkable enhancement or suppression of population transfer can be realized through the spontaneous emission constructive or destructive quantum interference even with a finite pulse area.

Recently, there is great interest in extending these studies to semiconductor nanostructures [22–27] for the possible implementation of optoelectronic devices. In the conduction band of semiconductor quantum structure, the confined electron gas exhibits atomiclike behaviors. The intersubband energies and electron wave function symmetries could be engineered, with the flexibility unknown in atomic systems, to suit particular requirements. For example, Binder [22] investigated theoretically the light-induced adiabatic population transfer of holes from the heavy-hole (hh) to the light-hole (lh) band in p-doped semiconductor quantum wells (QWs). In additions, the coherent electron population transfer could also be achieved in coupled asymmetric semiconductor quantum dots [23,27] with STIRAP.

In the present paper, we design an n-doped asymmetric AlGaAs/GaAs double QW with a continuum, which has four subbands with a closely separated excited doublets, as shown in Fig. 1. We will investigate the dynamics behavior of the electrons in this system and find the conditions when efficient population transfer could occur. In our structure, the quantum tunneling to the continuum from the excited doublet could give rise to the Fano-type interference [28], which has been observed experimentally in semiconductor intersubband transitions [29], and the sign of quantum interference (constructive or destructive) in optical absorption can be reversed by varying the direction of tunneling from the excited doublet to a common continuum [30]. Therefore, we will analyze the controllability of the coherent electron population transfer in the four-subband double QW structure via tuning the sign of quantum interference due

* Corresponding authors.
E-mail addresses: niuyp@mail.siom.ac.cn (Y. Niu), sqgong@ecust.edu.cn (S. Gong).

0030-4018/$ – see front matter.
doi:10.1016/j.optcom.2011.02.064

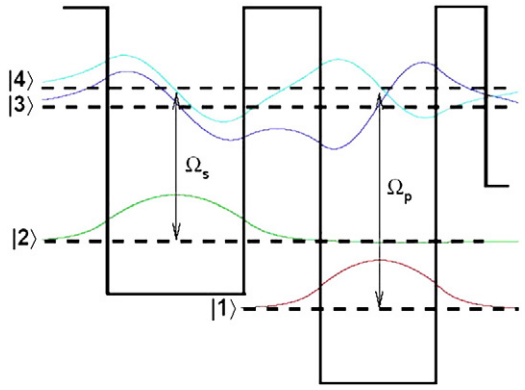

Fig. 1. Conduction subbands of the asymmetric double QW. It consists of two wells and a collector region separated by thin tunneling barriers. The dash lines denote the energy subbands and the solid curves represent the corresponding wave functions.

to resonant tunneling, the splitting of the excited doublet (the coupling strength of the tunneling), and the Fano-type interference. By numerically solving the motion equations of element moments, the almost complete electron population transfer from the initial subband to the target subband could be realized due to the constructive interference by suitably adjusting the structure parameters.

2. The model and basic equations

The n-doped asymmetric GaAs/AlGaAs double QW under consideration is shown in Fig. 1. One $Al_{0.07}Ga_{0.93}As$ QW with thickness of 8.3 nm is separated from a 6.9 nm GaAs QW by a $Al_{0.32}Ga_{0.68}As$ potential barrier with thickness of d. On the right side of right well is a 3.4 nm thin $Al_{0.32}Ga_{0.68}As$ barrier, which is followed by a thick $Al_{0.16}Ga_{0.84}As$ layer. In this structure, if we choose $d=4.8$ nm, the energies of the ground subbands $|1\rangle$ and $|2\rangle$ for the two wells are obtained as 51.53 meV and 97.78 meV, respectively. Two closely spaced delocalized upper levels $|3\rangle$ and $|4\rangle$, with the energies 191.30 meV and 203.06 meV respectively, are created by mixing the first excited subband of the shallow well $|se\rangle$ and the first excited subband of the right deep well $|de\rangle$ by tunneling. The dashed lines denote the energy subbands and the solid curves represent the corresponding wave functions. The subband $|1\rangle$ and subbands $|3\rangle$ and $|4\rangle$ are coupled by the pump laser (the amplitude E_p and center frequency ω_p) with the Rabi frequencies $\Omega_p=\mu_{13}E_p/\hbar$ and $k\Omega_p=\mu_{14}E_p/\hbar$, respectively. The subband $|2\rangle$ and subbands $|3\rangle$ and $|4\rangle$ are coupled by the Stokes laser (the amplitude E_s and center frequency ω_s) with the Rabi frequencies $\Omega_s=\mu_{23}E_s/\hbar$ and $q\Omega_s=\mu_{24}E_s/\hbar$, respectively. The Rabi frequencies of the pump and Stokes pulses are assumed to be Gaussian shape with the amplitude envelopes of the form $\Omega_p=\Omega_{p0}\exp[-(t-T_p)^2/\tau^2]$ and $\Omega_s=\Omega_{s0}\exp[-(t-T_s)^2/\tau^2]$, respectively, where τ is the pulse duration, and $T_p(T_s)$ is the time delay of pump (Stokes) pulse. Moreover, Ω_{p0} and Ω_{s0} are the peak values of the Rabi frequencies of pump and Stokes pulses, respectively. For simplicity, we denote $\Omega_{p0}=\Omega_{s0}$ in the following discussion. In addition, $k=\mu_{14}/\mu_{13}$ and $q=\mu_{24}/\mu_{23}$ present the ratios between the intersubband dipole moments of the relevant transitions, and $\mu_{ij}(i,j=1-4,i\neq j)=\vec{\mu}_{ij}\cdot\vec{e}_L$ ($\vec{e}_L$ is the unit polarization vector of the corresponding laser field) denotes the dipole moment for the transition between subbands $|i\rangle$ and $|j\rangle$.

In the four-subband QW structure, the direct optical resonance $|1\rangle(|2\rangle)\rightarrow|c\rangle$ ($|c\rangle$ is the continuum subband) is much weaker than those mediate resonance paths $|3\rangle(|4\rangle)\rightarrow|1\rangle$ and $|3\rangle(|4\rangle)\rightarrow|2\rangle$, thus the influence of the direct transition $|1\rangle(|2\rangle)\rightarrow|c\rangle$ could be ignored [28]. In addition, when the electron sheet density smaller than 10^{12} cm^{-2} and with the actual temperature at 10 K, the electron–electron effects have very small influence in our results. Under these assumptions, following the standard processes [31], the system dynamics could be described by the motion equations for the matrix elements in a rotating frame:

$$\dot{\rho}_{11}=ik\Omega_p(\rho_{41}-\rho_{14})+i\Omega_p(\rho_{31}-\rho_{13})+\gamma_{41}\rho_{44}+\gamma_{31}\rho_{33}+\gamma_2\rho_{22}+\frac{\eta}{2}(\rho_{34}+\rho_{43}), \tag{1}$$

$$\dot{\rho}_{22}=iq\Omega_s(\rho_{42}-\rho_{24})+i\Omega_s(\rho_{32}-\rho_{23})+\gamma_{42}\rho_{44}+\gamma_{32}\rho_{33}-\gamma_2\rho_{22}+\frac{\eta}{2}(\rho_{34}+\rho_{43}), \tag{2}$$

$$\dot{\rho}_{33}=i\Omega_p(\rho_{13}-\rho_{31})+i\Omega_s(\rho_{23}-\rho_{32})-\gamma_3\rho_{33}-\frac{\eta}{2}(\rho_{34}+\rho_{43}) \tag{3}$$

$$\dot{\rho}_{44}=ik\Omega_p(\rho_{14}-\rho_{41})+iq\Omega_s(\rho_{24}-\rho_{42})-\gamma_4\rho_{44}-\frac{\eta}{2}(\rho_{34}+\rho_{43}) \tag{4}$$

$$\dot{\rho}_{12}=-\left[i\left(\Delta_p-\Delta_s\right)+\frac{\Gamma_{12}}{2}\right]\rho_{12}+ik\Omega_p\rho_{42}+i\Omega_p\rho_{32}-iq\Omega_s\rho_{14}-i\Omega_s\rho_{13} \tag{5}$$

$$\dot{\rho}_{13}=-\left(i\Delta_p+\frac{\Gamma_{13}}{2}\right)\rho_{13}+ik\Omega_p\rho_{43}-i\Omega_s\rho_{12}+i\Omega_p(\rho_{33}-\rho_{11})-\frac{\eta}{2}\rho_{14} \tag{6}$$

$$\dot{\rho}_{14}=-\left[i\left(\Delta_p-\omega_{43}\right)+\frac{\Gamma_{14}}{2}\right]\rho_{14}+i\Omega_p\rho_{34}-iq\Omega_s\rho_{12}+ik\Omega_p(\rho_{44}-\rho_{11})-\frac{\eta}{2}\rho_{13} \tag{7}$$

$$\dot{\rho}_{23}=-\left(i\Delta_s+\frac{\Gamma_{23}}{2}\right)\rho_{23}-i\Omega_p\rho_{21}+iq\Omega_s\rho_{43}+i\Omega_s(\rho_{33}-\rho_{22})-\frac{\eta}{2}\rho_{24} \tag{8}$$

$$\dot{\rho}_{24}=-\left[i(\Delta_s-\omega_{43})+\frac{\Gamma_{24}}{2}\right]\rho_{24}-ik\Omega_p\rho_{21}+i\Omega_s\rho_{34}-iq\Omega_s(\rho_{22}-\rho_{44})-\frac{\eta}{2}\rho_{23} \tag{9}$$

$$\dot{\rho}_{34}=-\left(-i\omega_{43}+\frac{\Gamma_{34}}{2}\right)\rho_{34}-ik\Omega_p\rho_{31}+i\Omega_p\rho_{14}-iq\Omega_s\rho_{32}+i\Omega_s\rho_{24}-\frac{\eta}{2}(\rho_{33}+\rho_{44}) \tag{10}$$

with $\rho_{ij}=\rho_{ij}^*$ and the electron conservation condition $\rho_{11}+\rho_{22}+\rho_{33}+\rho_{44}=1$. Here, $\omega_{ij}(i,j=1-4,i\neq j)=\omega_i-\omega_j$ is the resonant frequency between subbands $|i\rangle$ and $|j\rangle$, and $\omega_i(i=1-4)$ is the frequency of the subband $|i\rangle$. $\omega_{43}=\omega_4-\omega_3$ is the energy splitting between levels $|4\rangle$ and $|3\rangle$, given by the coherent coupling strength of the electron tunneling. $\Delta_p=\omega_p-\omega_{31}$ is the detuning of the pump laser from the resonant transition $|1\rangle\rightarrow|3\rangle$, and $\Delta_s=\omega_s-\omega_{32}$ is the detuning between the frequency of the Stokes laser and the transition frequency ω_{32}. The population decay rates and dephasing decay rates are added phenomenologically in the above density-matrix. The population decay rates for subband $|i\rangle$ denoted by γ_i, are due primarily to longitudinal-optical (LO) phonon emission events at low temperature. The total decay rates ($\Gamma_{ij}(i\neq j)$) are given by $\Gamma_{12}=\gamma_2+\gamma_{12}^{dph}$, $\Gamma_{13}=\gamma_3+\gamma_{13}^{dph}$ ($\gamma_3=\gamma_{31}+\gamma_{32}$), $\Gamma_{14}=\gamma_4+\gamma_{14}^{dph}$ ($\gamma_4=\gamma_{41}+\gamma_{42}$), $\Gamma_{23}=\gamma_2+\gamma_3+\gamma_{23}^{dph}$, $\Gamma_{24}=\gamma_2+\gamma_4+\gamma_{24}^{dph}$, $\Gamma_{34}=\gamma_3+\gamma_4+\gamma_{34}^{dph}$, where the pure dephasing decay rate $\gamma_{ij}^{dph}(i\neq j)$ is determined by electron–electron effects, interface roughness, and phonon scattering process. For temperature up to 10 K with electron sheet densities smaller than $10^{12}cm^{-2}$, the dephasing rates could be estimated [32] to be $\hbar\gamma_{13}^{dph}=$

$\hbar\gamma_{23}^{dph}=0.32$ meV, $\hbar\gamma_{14}^{dph}=\hbar\gamma_{24}^{dph}=0.30$ meV, $\hbar\gamma_{34}^{dph}=0.31$ meV and $\hbar\gamma_{12}^{dph}=0.47\times10^{-9}$meV. For our QWs considered above, the population decay rates turn out to be $\hbar\gamma_3=1.58$ meV, $\hbar\gamma_4=1.50$ meV, and $\hbar\gamma_2=2.36\times10^{-9}$meV.

The Fano-type interference factor $\eta=\sqrt{\gamma_3\gamma_4}$ represents the mutual coupling of subbands $|3\rangle$ and $|4\rangle$ arising from the tunneling to the continuum through the thin barrier. We define $\varepsilon=\eta/\sqrt{\Gamma_{13}\Gamma_{14}}$ for assessing the strength of the cross coupling, where the limit values $\varepsilon=0$ and $\varepsilon=1$ correspond to no interference (negligible coupling between $|3\rangle$ and $|4\rangle$) and perfect interference (no dephasing), respectively. From the above estimates, we obtain $\varepsilon=0.83$, which could be augmented by decreasing the temperature which generally leads to smaller dephasing rates γ_{ij}^{dph}.

3. The coherent electron population transfer

For the QW structure we consider in Fig. 1, there is the resonant tunneling between the close first excited subbands of the two QWs, which induces the dressed excited doublet $|3\rangle$ and $|4\rangle$. The quantum tunneling to the continuum from the excited doublet leads to the Fano-type interference. The direction of tunneling can be inverted by reversing the position of the barrier between the continuum and the well (the deep or shallow well), which would cause a change sign in the transition matrix element. The change of quantum interference would influence the system dynamics, such as tunneling induced transparency [30,32]. Besides, the coupling strength of tunneling is represented by the energy splitting of the excited doublet, which could be adjusted by varying the height and width of tunneling barrier *d*. Therefore, we will investigate the achievement of perfect coherent electron population transfer in an asymmetric semiconductor QW system interacting with a counterintuitively ordered pulses (i.e., the Stokes pulse precedes the pump pulse), by properly adjusting the parameters of QW structure, such as the sign of quantum interference due to resonant tunneling, the splitting of the excited doublet (the coupling strength of the tunneling), as well as the coupling strength of Fano-type interference.

Initially, if the electron dephasing and population decays of the excited doublet are not taken into account, the four-subband QW structure is similar to the excited-doublet four-level atom system [20,21]. In Ref. [20], the existence of dark states is possible with the contribution from the excited doublet, and the behavior of adiabatic passage is demonstrated that it depends crucially on detunings between the laser frequencies and the atomic transition frequency. When the pump and Stokes fields keep two-photon resonance, but are not tuned at the midpoint of the excited doublet, only one dark state exists, which is

$$|\phi_0\rangle=\cos\theta|1\rangle-\sin\theta|2\rangle, \tag{11}$$

where $\tan\theta=\Omega_p/\Omega_s$, and θ is the mixing angle used in standard STIRAP. In the adiabatic regime, a complete population transfer from an initial state $|1\rangle$ to another target state $|2\rangle$ can be realized with counterintuitively ordered pulses, just as in the three-level Λ system [1]. However, when both pump and Stokes fields are tuned to the center of the two upper levels, there exist two dark states, one is the trapped state of Eq. (11), and the other is

$$|\phi_1\rangle=\sin\theta\sin\varphi|1\rangle+\cos\theta\sin\varphi|2\rangle+\frac{\cos\varphi}{\sqrt{2}}(|3\rangle-|4\rangle), \tag{12}$$

where $\tan\varphi=\omega_{43}/2/\sqrt{2\left[\Omega_s^2+\Omega_p^2\right]}$, and φ is an additional mixing angle related to the energy separation of the excited doublet. For a counterintuitively ordered pulses, due to the nonadiabatic coupling between the two degenerate states $|\phi_0\rangle$ and $|\phi_1\rangle$, the system vector $|\Psi(\infty)\rangle$ is a mixture of the two bare states $|1\rangle$ and $|2\rangle$, as follows

$$|\Psi(\infty)\rangle=\sin\gamma_f(\infty)|1\rangle-\cos\gamma_f(\infty)|2\rangle, \tag{13}$$

where $\gamma_f=\int_{-\infty}^{t}(d\theta/dt')\sin\varphi dt'$ is the Berry phase [20]. Obviously, an arbitrary superposition of atomic states can be prepared when ω_{43} is comparable to Ω_p and Ω_s. It can also be seen from Eq. (13) that, if ω_{43} is much larger than Ω_p and Ω_s, then φ nearly equals $\pi/2$, and almost no population transfer can occur; while if the energy separation of the doublet ω_{43} is far smaller than the peak Rabi frequencies Ω_p and Ω_s, then φ is nearly equal to zero, and the population transfer behaves almost in the same manner as that in the Λ-type three-level system.

However, the electron population decays and dephasing rates in semiconductor QWs structure should be considered, which is very important in many dynamics processes. In this condition, we could not derive the expressions for the dark states to achieve the complete adiabatic population transfer. However, by solving the density matrix equations [Eqs. (1)–(10)] numerically, we can obtain the dynamics behavior of electron populations in the four subband QW structure with a continuum coupled by the counterintuitively ordered pulses with a finite pulse area.

In order to investigate the effects of resonant tunneling with reversed sign on the population dynamics, we present the time evolution of populations in the four subband QWs with a continuum adjacent to the shallow well (similar to Fig. 1b in Ref. [30], which is not shown here) in Fig. 2(a) and the deep well (Fig. 1) in Fig. 2(b). The parameters of the laser fields are taken as $\hbar\Omega_{p0}=\hbar\Omega_{s0}=2.6$ meV, $\tau=10$ meV^{-1}, $T_s=30$ meV^{-1}, and $T_p=50$ meV^{-1}, and the Rabi frequencies are much smaller than the energy splitting of the excited doublet $\hbar\omega_{43}=11.76$ meV. It can be seen from Fig. 2 that the electron

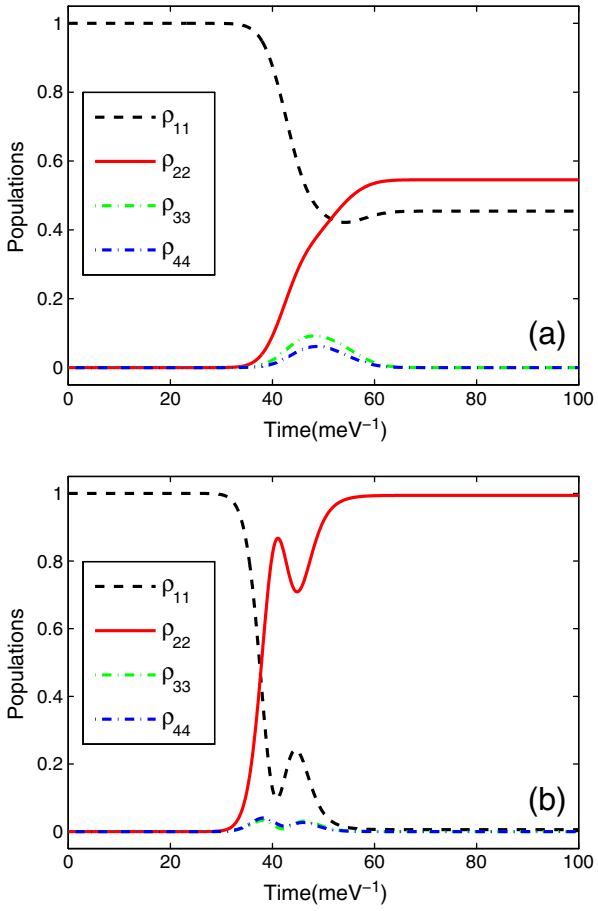

Fig. 2. The time evolution of the populations in the four subbands ρ_{11} (dash line), ρ_{22} (solid line), ρ_{33} (dot-dash line) and ρ_{44} (dot-dash line) with the laser fields tuned at the middle point of the upper two subbands under different values of the dipole ratios $k=0.70$ and $q=0.90$ in (a), and $k=-0.70$ and $q=0.90$ in (b) with $\hbar\Omega_{p0}=\hbar\Omega_{s0}=2.6$ meV, $\tau=10$ meV^{-1}, $T_s=30$ meV^{-1}, $T_p=50$ meV^{-1}, $\hbar\omega_{43}=11.76$ meV, $\hbar\gamma_3=1.58$ meV, $\hbar\gamma_4=1.50$ meV and $\hbar\gamma_2=2.36\times10^{-9}$meV.

population transfer is dramatically modified by the sign of the interference (destructive or constructive) due to the direction reverse of resonant tunneling. In the case of Fig. 2(a), only a part of electrons in subband $|1\rangle$ could transfer to subband $|2\rangle$. In this condition, the dipole moments between the two upper subbands and each of the two lower subbands are parallel (the ratios of the dipole moments be calculated to be $k=0.70$ and $q=0.90$). As a result, the interference via spontaneous decay pathways is destructive, which prevents the electron population in subband $|1\rangle$ from being excited by the pump field. That is to say, for the pump and Stokes fields with the same amplitudes and tuned midway between the excited doublet, the efficient electron population transfer could not be achieved in the asymmetric QW structure with the continuum adjacent to the shallow well. However, with constructing the continuum adjacent to the deep well through the thin barrier as shown in Fig. 1, the transition matrix elements from the excited doublet to each of the lower subbands become antiparallel, and the ratios of the transition matrix elements change to be $k=-0.70$ and $q=0.90$. Thus, the constructive interference via resonant tunneling which suppresses the effects of the quantum coherence of spontaneous decays, when the pump and Stokes fields keep the two-photon resonance and are tuned at the center of the excited doublet. Therefore, the perfect electron population transfer could be achieved [as shown in Fig. 2(b)] by reversing the sign of the interference induced by resonant tunneling, i.e., change the directions of the common continuum [30].

Fig. 3 represents the time evolution of the populations in the four subbands with different splittings of the excited doublet. For our structure, the splitting indicates the coupling strength of resonant tunneling, which could be controlled by adjusting the height and width of the tunneling barrier. Compared with Fig. 2(b), we just change the width of tunneling barrier d, while keeping other structure parameters fixed. It is can be seen that, the perfect electron population transfer occurs when the splitting ω_{43} is much smaller [$\hbar\omega_{43}=5.93$ meV in Fig. 3(a)]. As further decreasing the splitting (even smaller than the peak Rabi frequencies Ω_p and Ω_s), the electron populations

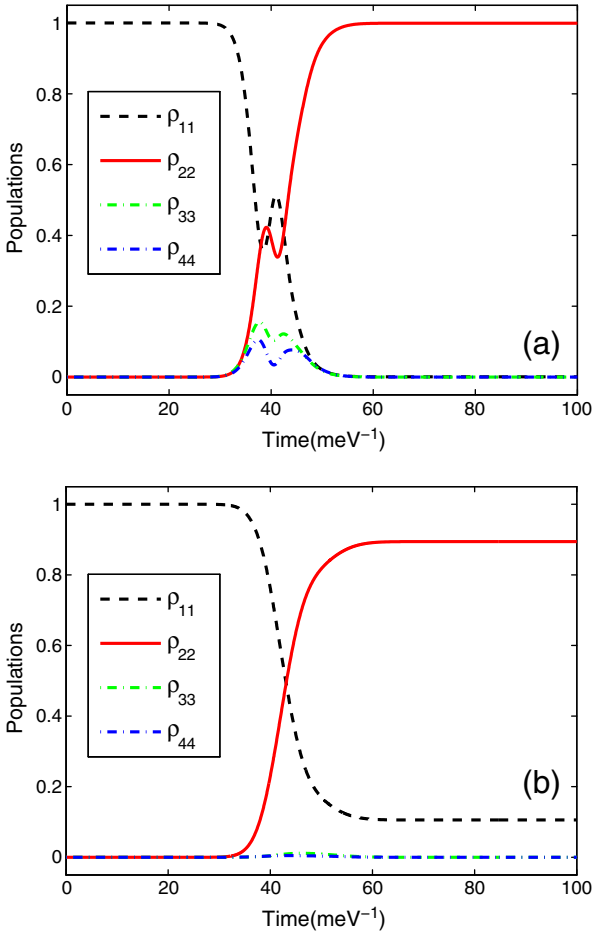

Fig. 3. The time evolution of the populations in the four subbands ρ_{11} (dash line), ρ_{22} (solid line), ρ_{33} (dot-dash line) and ρ_{44} (dot-dash line) with the laser fields tuned at the middle point of the upper two subbands under different splittings of the doublet, (a) $\hbar\omega_{43}=5.93$meV, $k=-0.59$ and $q=1.20$, (b) $\hbar\omega_{43}=25.38$meV, $k=-0.61$ and $q=0.56$. The other parameters are the same as in Fig. 2(b).

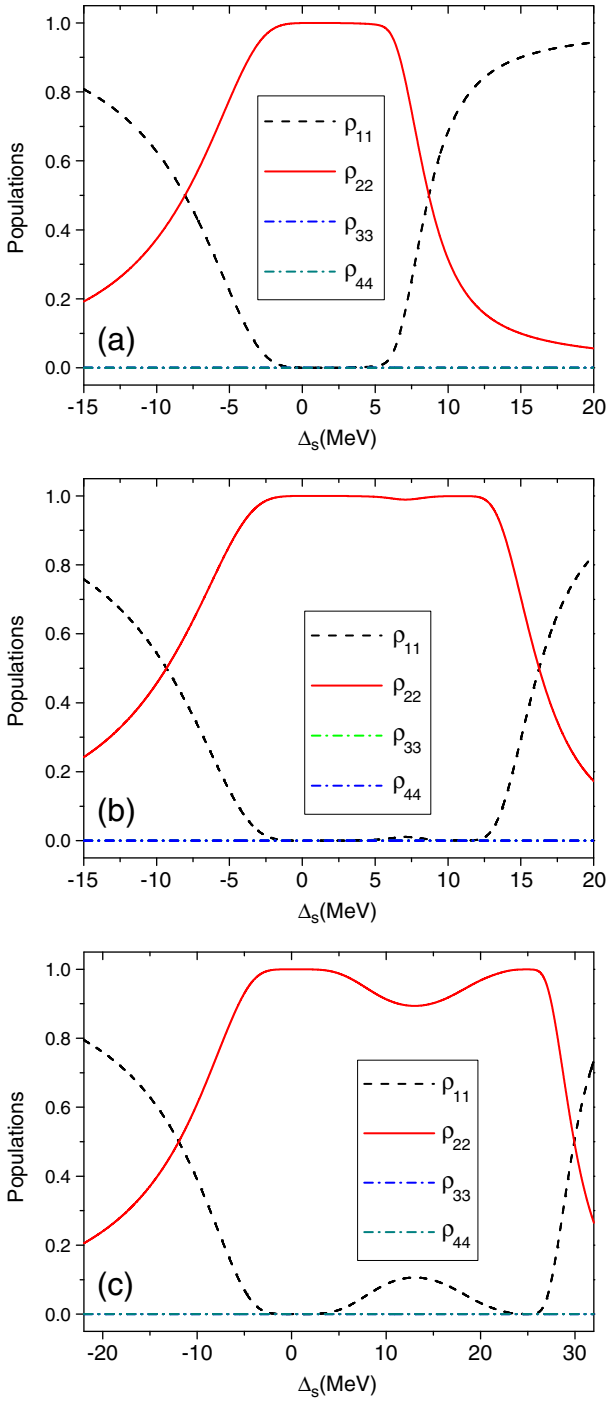

Fig. 4. The final populations in the four subbands ρ_{11} (dash line), ρ_{22} (solid line), ρ_{33} (dot-dash line) and ρ_{44} (dot-dash line) as a function of the one-photon detunings of the pump and Stokes lasers $\Delta_p=\Delta_s$, with different splittings of the doublet, (a) $\hbar\omega_{43}=5.93$ meV, $k=-0.59$ and $q=1.20$, (b) $\hbar\omega_{43}=11.76$ meV, $k=-0.70$ and $q=0.90$, (c) $\hbar\omega_{43}=25.38$ meV, $k=-0.61$ and $q=0.56$. The other parameters are the same as in Fig. 2(b).

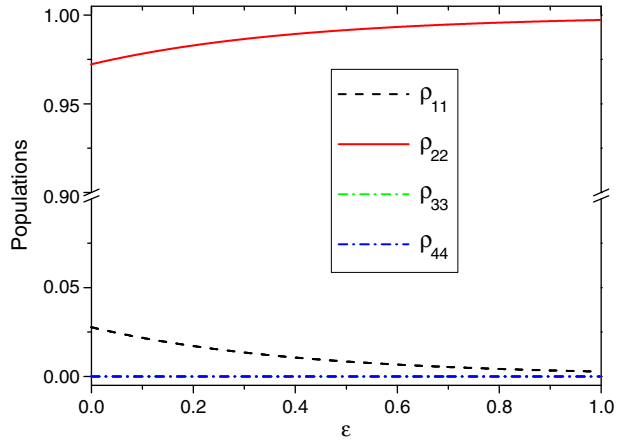

Fig. 5. The final populations in the four subbands ρ_{11} (dash line), ρ_{22} (solid line), ρ_{33} (dot-dash line) and ρ_{44} (dot-dash line) as a function of the Fano-type interference factor ε. The other parameters are the same as in Fig. 2(b).

could also be completely transferred from the initial subband $|1\rangle$ to the target subband $|2\rangle$, which is not shown here. While with the increase of the splitting of the excited doublet, the efficiency of electron population transfer becomes lower, such as in Fig. 3(b) with $\hbar\omega_{43}=25.38$ meV. The results are in accordance with the analysis from Eq. (13), which could also be well understood from the final populations as a function of the one-photon detuning under different values of the splittings of excited doublet, as shown in Fig. 4.

As seen from Fig. 4 (a) and (b), nearly complete electron population transfer from the initial subband $|1\rangle$ to the target subband $|2\rangle$ occurs at the middle point of the two one-photon resonances with smaller splitting of excited doublet ($\hbar\omega_{43}=5.93$ meV and $\hbar\omega_{43}=11.76$ meV). As the energy splitting of the excited doublet becomes much larger ($\hbar\omega_{43}=25.38$ meV) than the laser field Rabi frequency, the electron population transfer efficiency at the middle point decreases with the limited pulse area. Moreover, in Fig. 4, we find that the population profiles with respect to the one-photo detunings $\Delta_p=\Delta_s$ are not symmetric. This asymmetry is due to the inequality of the intersubband transitions with the same incident pulse, i.e., $|k|,|q|\neq 1$. However, an almost complete electron population transfer could be controlled simply by appropriately adjusting the energy splitting of the excited doublet, i.e., the width or the height of the tunneling barrier.

Moreover, the effects of the strength or quality of the Fano-type interference on electron population transfer behavior could be clearly seen from Fig. 5. From this figure, we can see that the population transfer efficiency increases as the strength of interference ε increasing. The reason is that, the increase of the strength of the interference, which means the decrease of the dephasing process, enhances the coherence from the constructive quantum interference. As from the expressions $\varepsilon=\sqrt{\gamma_3\gamma_4}/\sqrt{\Gamma_{13}\Gamma_{14}}$ ($\Gamma_{13}=\gamma_3+\gamma_{13}$ and $\Gamma_{14}=\gamma_4+\gamma_{14}$), the strength of cross coupling ε varies dependently on the dephasing rates γ_{13} and γ_{14}, which are sensitive to the environment temperature. We could decrease the temperature to reduce the effect of dephasing rates. As a result, we can achieve an almost complete electron population transfer via properly increasing the strength of the cross coupling, which could be achieved by decreasing the temperature.

It should be noted that a change in the splitting of excited doublet may be connected to a slight change in dephasing and decay rates. However, via properly adjusting other physical variables such as temperatures, interface roughness scattering and so on, we believe that some experimental scientists have adequate wisdom to keep them unchanged. As a matter of fact, we have tried several other values of dephasing rates $\gamma_{12}^{dph},\gamma_{13}^{dph},\gamma_{14}^{dph},\gamma_{23}^{dph},\gamma_{24}^{dph},\gamma_{34}^{dph}$, and population decay rates $\gamma_2,\gamma_3,\gamma_4$ with the changes of the splitting of the excited doublet, similar coherent population transfer behavior could also be obtained for these different choices. In view of this, for comparison, we keep dephasing and decay rates fixed in Figs. 3 and 4.

In addition, we want to mention about the superposition state between subband $|1\rangle$ and $|2\rangle$. We display in Fig. 6 that, with the much weaker laser fields, the confined electrons can stay half in subband $|1\rangle$ and half in subband $|2\rangle$. But this doesn't mean we could get the maximum superposition state, because from Fig. 6(b), which presents the time evolution of the coherence between subband $|1\rangle$ and $|2\rangle$ ρ_{12}, the final steady values of the coherence $Re\rho_{12}$ ($Im\rho_{12}$) are not ± 0.5 (0). Therefore, the superposition state in our case is incoherent because the incoherence processes of the electron population decays and dephasing rates in semiconductor QWs structure have been considered.

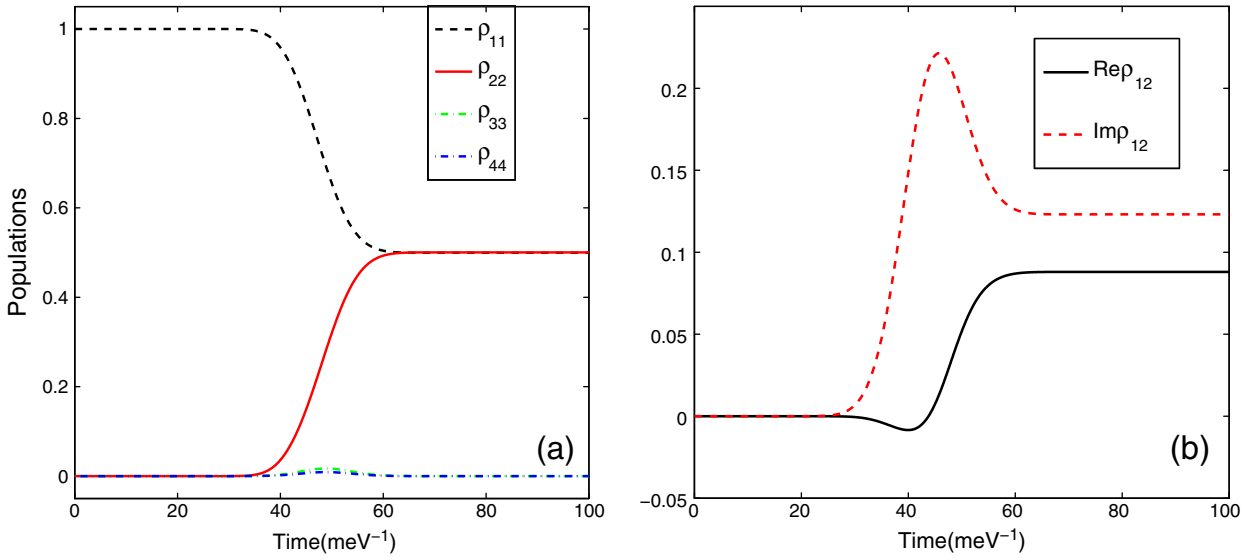

Fig. 6. (a) The time evolution of the populations in the four subbands ρ_{11} (dash line), ρ_{22} (solid line), ρ_{33} (dot-dash line) and ρ_{44} (dot-dash line) with the laser fields tuned at the middle point of the upper two subbands under different splittings of the doublet with $\hbar\Omega_{p0}=\hbar\Omega_{s0}=0.827$ meV. (b) The time evolution of the coherence ρ_{12}. The other parameters are the same as in Fig. 2(b).

4. Conclusions

In conclusion, we have investigated the controllability of coherent electron population transfer in an asymmetric double QW structure with a common continuum interacting with counterintuitively ordered pulses. Based on the numerical results of the motion equations of element moments, the perfect electron population transfer could be achieved by efficiently optimizing the semiconductor QW structure parameters, such as the direction and the coupling strength of the tunneling from the excited doublet to the common continuum, and the coupling strength of the Fano-type interference. It is more practical to control the population transfer behavior in the QW systems than in the atomic systems because of its flexible design and the controllable interference strength.

Acknowledgments

This work is supported by the National Natural Sciences Foundation of China (Grant Nos. 60708008, 10874194, 60978013, and 60921004), and the Key Basic Research Foundation of Shanghai (Grant No. 08JC1409702).

References

[1] K. Bergmann, H. Theuer, B.W. Shore, Rev. Mod. Phys. 70 (1998) 1003.
[2] N.V. Vitanov, M. Fleischhauer, B.W. Shore, K. Bergmann, Adv. At. Mol. Opt. Phys. 46 (2001) 55.
[3] M. Weitz, B.C. Young, S. Chu, Phys. Rev. A 50 (1994) 2438.
[4] A.S. Parkins, P. Marte, P. Zoller, O. Carnal, H.J. Kimble, Phys. Rev. A 51 (1995) 1578.
[5] N.V. Vitanov, K.A. Suominen, B.W. Shore, J. Phys. B At. Mol. Opt. Phys. 32 (1999) 4535.
[6] R. Unanyan, M. Fleischhauer, B.W. Shore, K. Bergmann, Opt. Commun. 155 (1998) 144.
[7] T. Pellizzari, S.A. Gardiner, J.I. Cirac, P. Zoller, Phys. Rev. Lett. 75 (1995) 3788.
[8] U. Gaubatz, P. Rudecki, M. Becker, S. Schiemann, M. Külz, K. Bergmann, Chem. Phys. Lett. 149 (1988) 463.
[9] P. Marte, P. Zoller, J.L. Hall, Phys. Rev. A 44 (1991) R4118.
[10] C.E. Carroll, F.T. Hioe, Phys. Rev. Lett. 68 (1992) 3523; Phys. Rev. A 47 (1993) 571.
[11] T. Nakajima, M. Elk, J. Zhang, P. Lambropoulos, Phys. Rev. A 50 (1994) R913.
[12] L.P. Yatsenko1, R.G. Unanyan, K. Bergmann, T. Halfmann, B.W. Shore, Opt. Commun. 135 (1997) 406.
[13] N.V. Vitanov, S. Stenholm, Phys. Rev. A 56 (1997) 741.
[14] R.G. Unanyan, N.V. Vitanov, S. Stenholm, Phys. Rev. A 57 (1998) 462.
[15] E. Paspalakis, M. Protopapas, P.L. Knight, Opt. Commun. 142 (1997) 34; J. Phys B 31 (1998) 775.
[16] R.G. Unanyan, N.V. Vitanov, B.W. Shore, K. Bergmann, Phys. Rev. A 61 (2000) 043408.
[17] T. Peters, T. Halfmanna, Opt. Commun. 271 (2007) 475.
[18] N.V. Vitanov, S. Stenholm, Phys. Rev. A 60 (1999) 3820.
[19] I.R. Sola, V.S. Malinovsky, Phys. Rev. A 68 (2003) 013412.
[20] S.Q. Jin, S.Q. Gong, R.X. Li, Z.Z. Xu, Phys. Rev. A 69 (2004) 023408.
[21] X.H. Yang, S.Y. Zhu, Phys. Rev. A 77 (2008) 063822.
[22] R. Binder, M. Lindberg, Phys. Rev. Lett. 81 (1998) 1477.
[23] U. Hohenester, F. Troiani, E. Molinari, G. Panzarini, C. Macchiavello, Appl. Phys. Lett. 77 (2000) 1864.
[24] J.F. Dynes, M.D. Frogley, J. Rodger, C.C. Phillips, Phys. Rev. B 72 (2005) 085323.
[25] S.G. Kosionis, A.F. Terzis, E. Paspalakis, Phys. Rev. B 75 (2007) 193305.
[26] H.Y. Hui, R.B. Liu, Phys. Rev. B 78 (2008) 155315.
[27] E. Voutsinas, J. Boviatsis, A. Fountoulakis, Phys. Stat. Sol. c 4 (2007) 439.
[28] U. Fano, Phys. Rev. 124 (1961) 1866.
[29] J. Faist, C. Sirtori, F. Capasso, S.N.G. Chu, L.N. Pfeiffer, K.W. West, Opt. Lett. 21 (1996) 985.
[30] J. Faist, F. Capasso, C. Sirtori, K.W. West, L.N. Pfeiffer, Nature 390 (1997) 589.
[31] S.E. Harris, Phys. Rev. Lett. 62 (1989) 1033.
[32] H. Schmidt, K.L. Campman, A.C. Gossard, A. Imamoğlu, Appl. Phys. Lett. 70 (1997) 3455.